

Unveiling the molecular environment of the enigmatic PeVatron candidate LHAASO J2108+5157

Iván Toledano-Juárez,^{a,*} Eduardo de la Fuente,^b Kazumasa Kawata,^c Daniel Tafoya,^d Miguel A. Trinidad,^e Mitsuyosh Yamagishi,^f Shunya Takekawa,^g Munehiro Ohnishi,^b Atsushi Nishimura,^h Sei Kato,^b Takashi Sako,^b Masato Takita,^b Hidetoshi Sanoⁱ and Ram K. Yadav^j

^aDoctorado en Ciencias en Física, CUCEI, Universidad de Guadalajara,
Blvd. Marcelino García Barragán 1420, 44430, Guadalajara, Jalisco, México

^bDepartamento de Física, CUCEI, Universidad de Guadalajara,
Blvd. Marcelino García Barragán 1420, 44430, Guadalajara, Jalisco, México

^cInstitute for Cosmic Ray Research, University of Tokyo
Kashiwa 277-8582, Japan

^dDepartment of Space, Earth, and Environment, Chalmers University of Technology,
Onsala Space Observatory, 439 92, Sweden

^eDepartamento de Astronomía, Universidad de Guanajuato
Apartado Postal 144, 36000, Guanajuato, Guanajuato, México

^fInstitute of Astronomy, Graduate School of Science, The University of Tokyo
2-21-1 Osawa, Mitaka, Tokyo 181-0015, Japan

^gDepartment of Applied Physics, Faculty of Engineering, Kanagawa University
3-27-1 Rokkakubashi, Kanagawa-ku, Yokohama, Kanagawa 221-8686, Japan

^hNobeyama Radio Observatory, National Astronomical Observatory of Japan, National Institutes of
Natural Sciences
462-2 Nobeyama, Minamimaki, Minamisaku, Nagano 384-1305, Japan

ⁱFaculty of Engineering, Gifu University
1-1 Yanagido, Gifu 501-1193, Japan

^jNational Astronomical Research Institute of Thailand (Public Organization)
260 Moo 4, T. Donkaew, A. Maerim, Chiangmai, 50180, Thailand

E-mail: ivan.toledano9284@alumnos.udg.mx

Abstract. We summarize the results of previous works in which we analyzed the molecular environment around the PeVatron candidate LHAASO J2108+5157, using $^{12,13}\text{CO}$ observations. We present evidence that the observed sub-PeV emission is produced in two molecular clouds as cosmic-ray targets ([FKT-MC]2022 and [FTK-MC]) with two different LSR velocities but with similar distances. We recalculate the distance of [FKT-MC]2022, obtaining a value of 1.6 kpc. In addition, we determined the energy required to produce the observed sub-PeV emission using the Naima package software.

38th International Cosmic Ray Conference (ICRC2023)
26 July - 3 August, 2023
Nagoya, Japan



*Speaker.

1. Introduction

PeVatrons are astronomical objects that act as natural particle accelerators capable of accelerating cosmic rays (CRs) up to PeV energies. The accelerated CRs can interact with the surrounding environment by hadronic(e.g. neutral pion decay) or leptonic(e.g. inverse Compton scattering) processes, giving place to gamma-ray emission with energies above 100 TeV. Their detection has been possible thanks to gamma-ray observatories such as LHAASO–KM2A [e.g. 1], HAWC (e.g [2]), and Tibet-AS γ (e.g. [3]). While some PeVatrons have already been associated with an astronomical object counterpart, the recently detected sub-PeV gamma-ray source LHAASO J2108+5157 (J2108 hereafter) [1, 4] is an exception. This enigmatic source is located at R.A. (J2000) = $21^h 08^m 52.8^s$; DEC (J2000) = $+51^{\circ} 57' 00''$, or $l = 92.30^{\circ}$; $b = 2.84^{\circ}$, towards the direction of Cygnus OB7 molecular cloud, suggesting that the its gamma-ray emission is hadronic in nature, in which the accelerated CRs interact with the molecular material in the environment.

In previous works ([5, 6]; hereafter paper I and paper II respectively), we analyzed $^{12,13}\text{CO}$ molecule line emission data towards the vicinity of J2108. Low resolution ($2.7'$) $^{12,13}\text{CO}$ ($J=2 \rightarrow 1$) data was obtained with the 1.8m Osaka Prefecture University (OPU) radio telescope (e.g. [7] and references therein), while higher resolution ($17.0''$) $^{12,13}\text{CO}$ ($J=1 \rightarrow 0$) data was obtained most recently with the 45m radio telescope of Nobeyama Radio Observatory (hereafter NRO-45m; e.g. [8]). Details of the observations and data reduction process are described in paper I (for low-resolution) and paper II (for high-resolution) respectively. CO emission is used as an indirect tracer for molecular hydrogen H₂, as the latter is not readily observable because of its higher-energy excitation transitions. Because ^{12}CO emission can become optically thick in molecular clouds, it becomes saturated and it is difficult to infer the whole molecular gas properties accurately. On the other hand, ^{13}CO emission could be optically thin, less susceptible to these opacity effects, making it possible to probe the inner regions of the molecular cloud, allowing us to better estimate the CO column density in order to calculate reliable physical parameters. Using archival atomic hydrogen HI 21cm data from the Dominion Radio Astrophysical Observatory (DRAO¹; [9]), we use CO and HI data to estimate the nucleon column density ($N(\text{H}) = N(\text{HI}) + 2N(\text{H}_2)$) in the vicinity of J2108.

In this work we present a summary of the analysis made in Paper I and II for the molecular environment around LHAASO J2108+5157. In Section 2 we describe the molecular clouds that we proposed to be associated with the sub-PeV gamma-ray emmission of LHAASO J2108+5157. The results and discussion are presented in Section 3, and the conclusions are summarized in Section 4.

2. Molecular clouds associated with LHAASO J2108+5157

J2108 was previously associated with the molecular cloud [MML2017]4607 [4] of the catalog of [10], detected by ^{12}CO ($J=1 \rightarrow 0$) with a LSR velocity (V_{LSR}) of $\sim -13 \text{ km s}^{-1}$. In paper I we proposed the molecular cloud [FKT-MC]2022 ($V_{\text{LSR}} \sim -3 \text{ km s}^{-1}$) to be another candidate to produce the observed sub-PeV gamma-ray emission of J2108, for which we favour a hadronic origin. This proposed molecular cloud was detected using optically thick OPU ^{12}CO ($J=2 \rightarrow 1$) emission and its physical parameters were estimated considering optically thin OPU ^{13}CO ($J=2 \rightarrow 1$) emission.

¹DRAO is part of the Canadian Galactic Plane Survey Project (CGPS). <https://www.cadc-ccda.hia-ihc.nrc-cnrc.gc.ca/en/search/#resultTableTab>

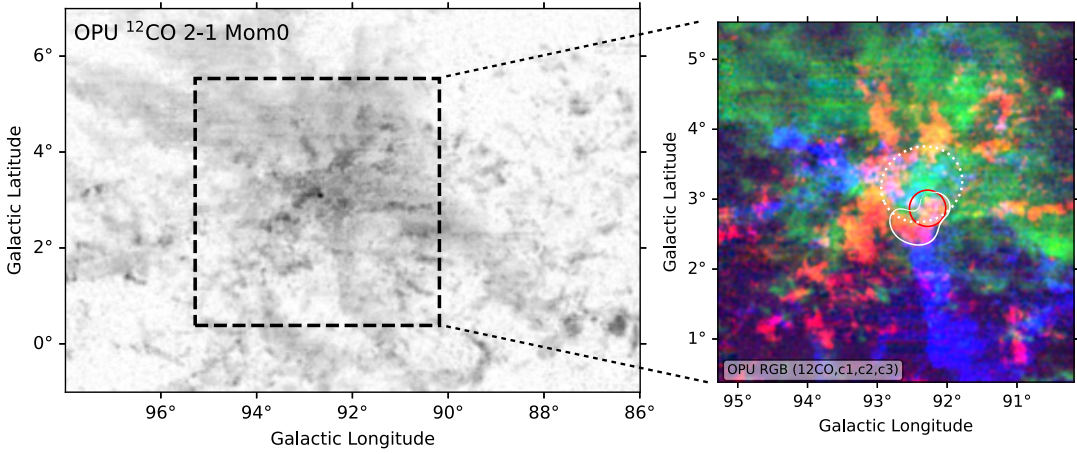


Figure 1: Molecular clouds associated to J2108. **Left:** Moment 0 map of the FOV of OPU ^{12}CO ($J=2\rightarrow 1$) observations towards Cygnus OB7 asociation [5], integrated between -100 and 80 km s^{-1} . The angular resolution of the map is $\sim 3'$. **Right:** RGB image as an inset of the left panel, in the vicinity of J2108. Colors show moment 0 maps associated with spectral components (see main text for details) C_1 (red), C_2 (green), and C_3 (blue), respectively. The red circle correspond to the 95% upper limit (radius 0.26 deg) of LHAASO J2108+5157. White dotted and solid lines denote the extension of molecular clouds [FKT-MC]2022 and FTK-MC, respectively.

However, the sensitivity of the ^{13}CO ($J=2\rightarrow 1$) OPU observations was not enough to study the spectral component at $V_{\text{LSR}} \sim -13 \text{ km s}^{-1}$ in the optically thin regime. In paper II, we used recent NRO-45m data to characterize a molecular cloud, labeled as [FTK-MC] ($V_{\text{LSR}} \sim -13 \text{ km s}^{-1}$) for the first time in the optically thin regime, which showed a remarkable agreement in morphology with *Fermi*-LAT data above 2 GeV aasociated with J2108 high energy (HE) gamma-ray counterpart 4FGL J2108.0+5155, reported by [11].

3. Results and Discussion for [FKT-MC]2022 and [FTK-MC]

In the left panel of Fig. 1 we present a moment 0 map of the field of view (FOV) of the OPU ^{12}CO ($J=2\rightarrow 1$) emission. In the vicinity of J2108, the molecular line emission presents three main spectral components, that we denote as C_1 , C_2 , and C_3 (paper II), with LSR velocities of -13 , -3 and $+9 \text{ km s}^{-1}$, respectively. We computed three moment 0 maps considering the following LSR velocity ranges: -20 to -8 km s^{-1} , -5 to -0 km s^{-1} , green), and 5 to 12 km s^{-1} , associated with spectral components C_1 , C_2 , and C_3 , respectively. We present the emission of each spectral component in a RGB image in the right panel of Fig. 1. The 95% upper limit (UL) of J2108 is denoted by a red circle, which intersects with the extension of the molecular clouds [FKT-MC]2022 and [FTK-MC], denoted by white dotted and solid lines, respectively. The position, V_{LSR} , and size of [FKT-MC]2022 is presented in Tab. 1. [FKT-MC]2022 is associated with spectral component C_2 , and is surrounded by molecular gas associated with component C_1 . Given the probability that both components correspond to molecular gas located at a similar distance (see Section 3.1), this could be indicating that [FKT-MC] lies in a cavity within the molecular cloud.

In the top panels of Fig. 2 we present a RGB image of the same spectral components, using the ^{12}CO ($J=1\rightarrow 0$) and ^{13}CO ($J=1\rightarrow 0$) NRO-45m data. The molecular cloud [FKT-MC] is delimited by a white solid line. However, the FOV of the NRO-45m observations does not cover all the extension of [FKT-MC]2022. We also show components C_1 and C_2 as contours in the corresponding bottom panels, in conjunction with a TS map, adapted from Fig. 3 of [11]) and obtained with *Fermi*–LAT above 2 GeV. With the higher resolution of the NRO-45m observations, we can see that [FKT–MC] has two substructures, that we denoted [FKT–MC]J2108 and [FKT–MC]HS (dashed and dotted ellipses, respectively), given their proximity to the positions of J2108 and HS, a HE gamma-ray source with a hard photon index, not included in the 4FGL catalog, and proposed by [11]. The position, V_{LSR} , and sizes of [FKT–MC]J2108 and [FKT–MC]HS are shown in Tab. 1. Considering both substructures, we estimated a size of ~ 0.55 deg for [FKT–MC] as a whole (paper II).

As previously mentioned, there is a remarkable correlation between the *Fermi*–LAT data and the CO emission distribution, particularly in the region of [FKT–MC], associated with spectral component C_1 . The CO emission is the brightest near the peak of the *Fermi*–LAT TS map. In addition, the molecular gas associated with [FKT–MC]2022 seems to also trace, albeit in a lesser way, the upper leftmost part of the extended *Fermi*–LAT data, in particular with the $^{13}\text{CO}(J=1\rightarrow 0)$. This correlation could indicate the possibility that the gamma-ray emission comes from the interaction (hadronic) between accelerated CRs and the molecular material of both clouds.

3.1 The distance to LHAASO J2108+5157

To estimate reliable physical parameters of the molecular cloud associated with J2108, a good estimate of the distance is essential. In the work of [4], J2108 was associated with the molecular cloud [MML2017]4607 of the catalog of [10], whose reported distance of 3.28 kpc was estimated using the kinematic distance method via the rotation curve model of Brand & Blitz [12], using the LSR velocity and coordinates of the molecular cloud as input. In paper II, we use instead the Bayesian calculator and algorithms of [13], which takes the V_{LSR} and position of a source as input, and determines a probability density function for the distance taking into account its probable association with near sources who have a parallax determined distance, the spiral arms of the Milky Way, or considering the kinematic distance. The inputs and results of these calculations are summarized in Tab. 1.

The results show that it is most probable that the molecular gas associated with component C_1 and C_2 is located at a similar distance of ~ 1.6 kpc, strongly influenced by the accurate measurement of the distance (1.63 kpc) to the near source G092.69+3.08 ($l=92.671^\circ$, $b=3.071^\circ$, $V_{\text{LSR}} = -5.0 \text{ km s}^{-1}$). Removing G092.69+3.08 from the parallax catalog in the algorithm results in a probable distance of ~ 2.8 kpc for spectral component C_1 , based on the kinematic distance to the source, while molecular gas with component C_2 would lie at a distance of ~ 1.3 kpc, associated with the Local Arm of the Milky Way. In both scenarios, it is most probable that the molecular gas associated with component C_3 is associated with the Local Arm at a distance of ~ 1.2 kpc. Ultimately we decide to use the estimated distance of 1.6 kpc for both [FKT–MC]2022 and [FKT–MC], given the agreement in morphology from molecular material from both clouds with the *Fermi*–LAT data.

Extracting the corresponding $^{12,13}\text{CO}$ ($J=2\rightarrow 1$) and $^{12,13}\text{CO}$ ($J=1\rightarrow 0$) spectra from the regions of [FKT–MC]2022 and [FKT–MC], respectively, in addition to the DRAO HI 21cm data, we estimate the physical parameters of the molecular clouds using the methods and considerations presented

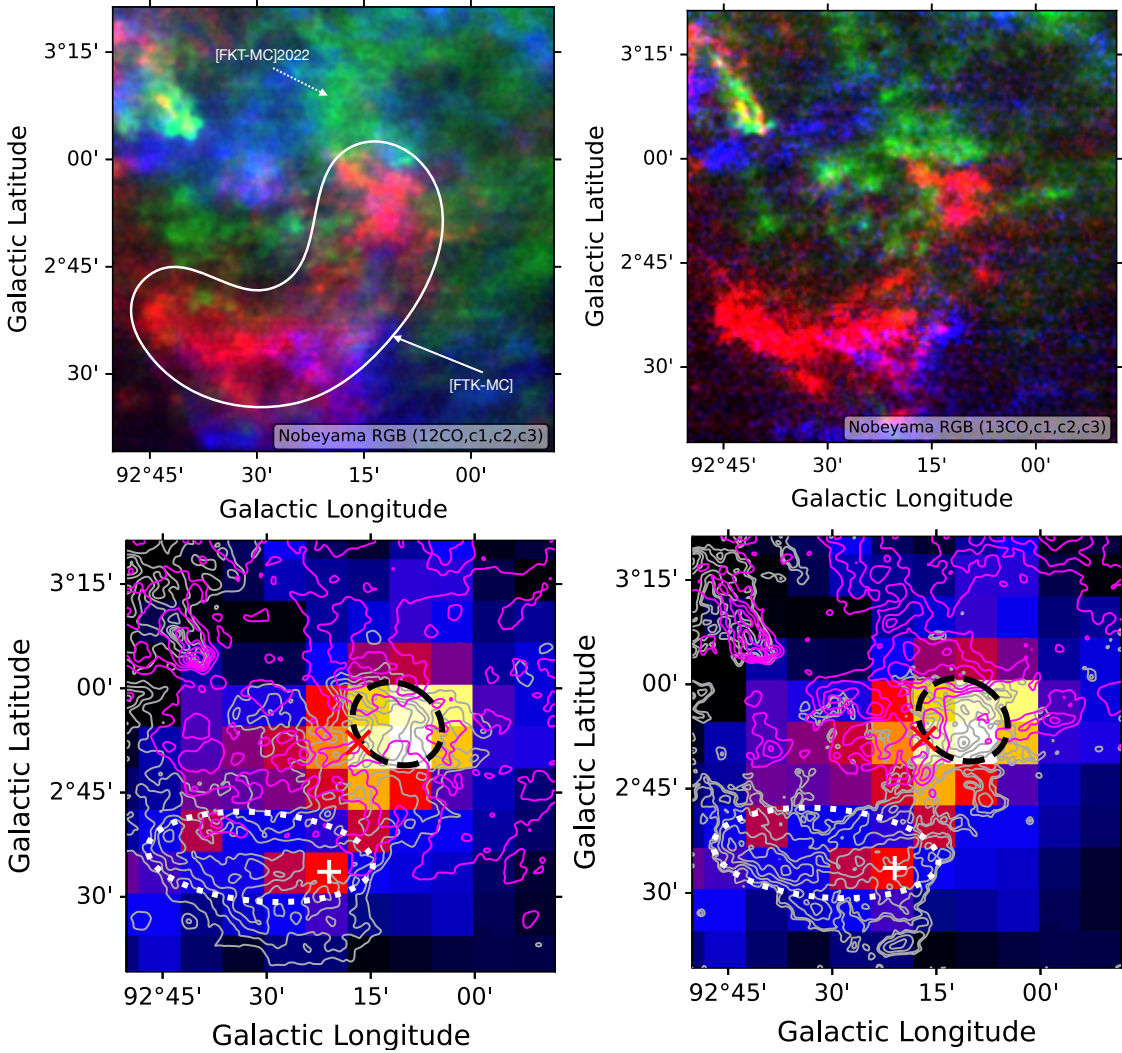


Figure 2: NRO-45m ^{12}CO (J=1→0) and ^{13}CO (J=1→0) observations. **Top:** RGB image of the spectral components of ^{12}CO (left) and ^{13}CO (right). The colors represent moment 0 maps integrated in the same LSR velocity ranges as right panel of Fig. 1. **Bottom:** *Fermi*-LAT TS map in color scale, adapted from Fig. 3 of [11], with ^{12}CO (J=1→0) (left) and ^{13}CO ^{12}CO (J=1→0) (right) moment 0 maps for spectral component C₁ (grey) and C₂ (magenta) overlaid as contours. The contours are [-4,4,5,8,12,16,20] times the rms value of 0.5 K km s⁻¹. The dashed black ([FTK-MC]2023/J2108) and white dotted ([FTK-MC]2023/HS) ellipses braces the two regions where the physical parameters were determined. The x and the cross indicate the central position of J2108 and HS respectively.

in Paper I and II. Assuming spherical symmetry, we consider a depth of 0.55 deg for [FTK-MC]. Given that the size of [FTK-MC] was computed using better constrained optically thin ^{13}CO (J=1→0) emission, we decide to use the same value for the depth of [FTK-MC]2022, for consistency. The nucleon number density n(H) was computed using the estimated distance of ~ 1.6 kpc to both sources. These considerations were not taken for [FTK-MC]2022 in Paper I. The derived physical parameters are listed in Tab. 2.

Table 1: Estimation of the distance to the molecular clouds [FKT-MC]2022 and [FTK-MC] using the Bayesian distance calculator of [13].

Cloud Name	l [deg]	b [deg]	Size [deg]	V_{LSR}^{**} [km s $^{-1}$]	Distance [kpc]	Probability	Association
[FKT – MC]2022	92.40	3.20	1.10 \pm 0.20	-2.9 \pm 0.1	1.6 \pm 0.1	0.59	Parallax
[FKT – MC]2022*	92.40	3.20	1.10 \pm 0.20	-2.9 \pm 0.1	1.3 \pm 0.2	0.92	Local Arm
[FTK – MC]J2108	92.20	2.90	0.34 \pm 0.01	-11.6 \pm 0.5	1.6 \pm 0.1	0.52	Parallax
[FTK – MC]J2108	92.20	2.90	0.34 \pm 0.01	7.2 \pm 0.5	1.2 \pm 0.3	0.50	Local Arm
[FTK – MC]J2108*	92.20	2.90	0.34 \pm 0.01	-11.6 \pm 0.5	2.7 \pm 0.7	0.47	Kinematic distance
[FTK – MC]HS	92.53	2.59	0.21 \pm 0.01	-13.2 \pm 0.5	1.6 \pm 0.1	0.43	Parallax
[FTK – MC]HS	92.53	2.59	0.21 \pm 0.01	8.8 \pm 0.5	1.2 \pm 0.3	0.46	Local Arm
[FTK – MC]HS*	92.53	2.59	0.21 \pm 0.01	-13.2 \pm 0.5	2.9 \pm 0.7	0.58	Kinematic distance

* Without considering G092.69+3.08 in the parallax sources catalog.

** The V_{LSR} of the sources were obtained using the corresponding ^{13}CO emission (Paper I and II).

Table 2: Physical parameters for the molecular clouds [FKT-MC]2022 and [FTK-MC], estimated using optically thin ^{13}CO emission.

Cloud Name	Distance [kpc]	$N(\text{H})^a$ [10^{21} cm^{-2}]	$n(\text{H})^{a,b}$ [cm^{-3}]	Size [deg]	$M(\text{HI} + \text{H}_2)$ [$10^3 M_{\odot}$]	T_{exc} [K]	W_p [10^{47} erg]	Cutoff [TeV]
[FTK-MC]	1.6 \pm 0.1	3.7 \pm 0.7	78 \pm 15	1.1 \pm 0.1	4.3 \pm 1.6	7.2 \pm 0.1	1.8 \pm 0.6	600 $^{+400}_{-200}$
[FKT – MC]2022	1.6 \pm 0.1	6.2 \pm 2.1	133 \pm 45	0.55 \pm 0.02	7.5 \pm 2.9	8.4 \pm 0.6	1.1 $^{+0.5}_{-0.3}$	600 $^{+300}_{-300}$

^a The column and number density of nucleons is calculated as $N(\text{H}) = 2N(\text{H}_2) + N(\text{HI})$ and $n(\text{H}) = 2n(\text{H}_2) + n(\text{HI})$, respectively.

^b The depth of [FTK-MC] of 0.55 deg was used for the estimation of the nucleon number density $n(\text{H})$ of [FKT-MC]2022.

The Naima² [14] package (version 0.10.0) in Python was employed to fit the spectra energy distribution (SED) of J2108 [4] at sub-PeV energies, considering the neutral pion decay hadronic process and using the obtained distance and nucleon number densities for both [FKT-MC]2022 and [FTK-MC] as input parameters. The hadronic modeling considers an exponential cutoff power law spectrum with a fixed spectral index of 2.0 [4]. The total required energy W_p and the energy cutoff of the cosmic ray proton population to reproduce the observed SED of J2108 are shown in Tab. 2 for each molecular cloud. A similar $W_p \sim 1.5 \times 10^{47}$ ergs is obtained for [FKT-MC]2022 and [FTK-MC], in agreement with what was reported in Paper II. A similar value of W_p could suggest that the molecular environments of both molecular clouds could contribute in a similar way to the observed sub-PeV gamma-ray emission, favouring the argument that both clouds are really located at a similar distance and are part of a same molecular structure.

We present the fitted SED of J2108 in Fig. 3, considering both hadronic (neutral pion decay) and leptonic (inverse Compton scattering) processes in the modelling. The leptonic modelling uses the same considerations of [4]. A total required energy of $W_e \sim 8.5 \times 10^{46}$ ergs for the electron population to reproduce the observed SED of J2108.

²<https://naima.readthedocs.io/en/latest/index.html>

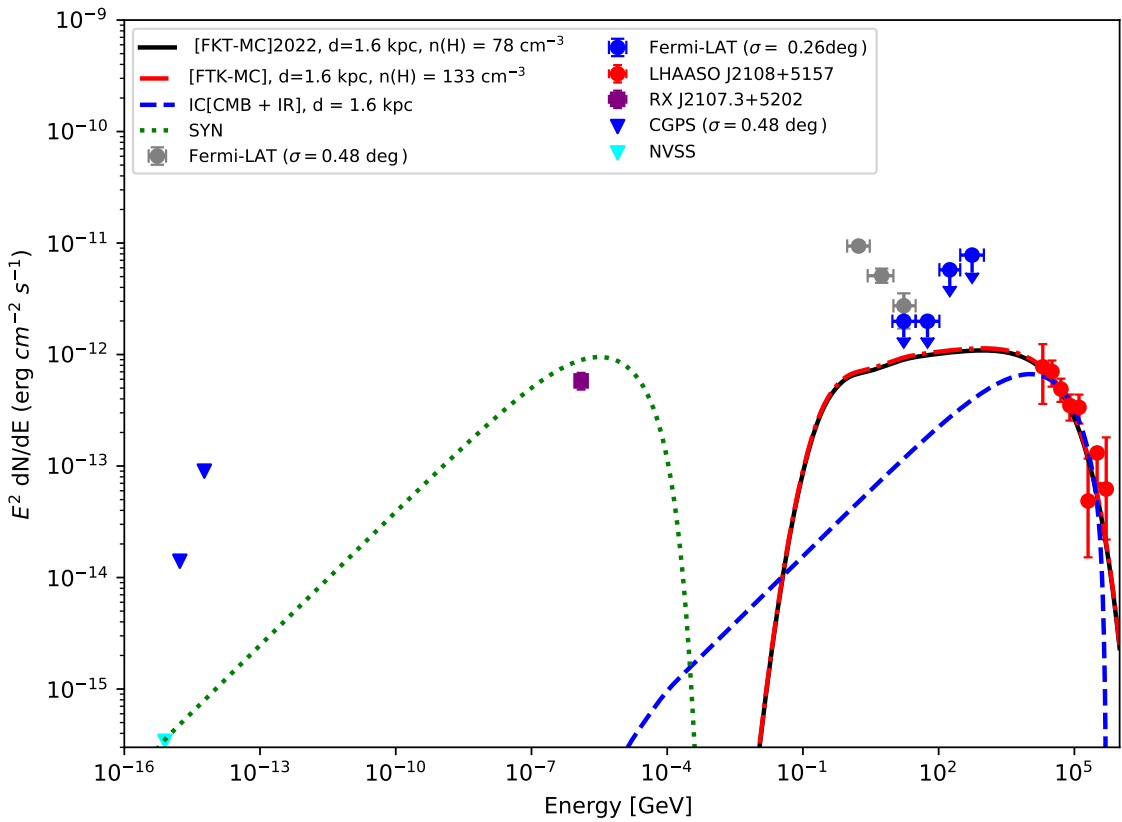


Figure 3: Spectral energy distribution of the LHAASO J2108+5157. The solid black and dashdotted red curves correspond to the hadronic modeling using the physical parameters of [FKT-MC]2022 and [FTK-MC], respectively. The green dotted curve is the spectral energy distribution expected from synchrotron radiation. The blue dashed curve represents the expected spectral energy from the inverse Compton effect, considering a CMB and IR seed photon field. For more details see Fig. 8 of Paper I.

4. Conclusions

Acknowledgments

The research summarized in this article was supported by the Inter-University Research Programme of the Institute for Cosmic Ray Research (ICRR), University of Tokyo (UTokyo), grant 2023i-F-005. EdelaF thanks the ICRR-UTokyo staff for several support during Sabbatical stay in 2021, and several academic stays between 2022 and 2023. IT-J gratefully acknowledges support from the Consejo Nacional de Ciencias y Tecnología, México grant 754851, and the Onsala Space Observatory during an academic visit in 2023. The authors are grateful for computational resources and technical support from the Centro de Análisis de Datos y Supercómputo of the Universidad de Guadalajara through the Leo-Atrox supercomputer. We thank xxx, J.L. Flores (UDG-CA-499), and an anonymous referee for their reviews and valuable comments to improve the manuscript.

References

- [1] Cao, Z., et al. 2021a, *Nature*, 594, 33
- [2] Abeysekara, A.U, et al. 2023, *Nucl. Instrum. Methods Phys. Res. A.*, 1052, 168253

- [3] Amenomori, M., et al., 2021c, PRL, 127, 031102
- [4] Cao, Z., et al. 2021b, ApJL, 919, L22
- [5] de la Fuente, E, Toledano-Juárez, I., Kawata, K., et al. 2023a, PASJ, 75, 546 (paper I)
- [6] de la Fuente, E, Toledano-Juárez, I., Kawata, K., et al. 2023b, A&A, 275, L5 (paper II)
- [7] Nishimura, A., Tokuda, K., Kimura, K., et al. 2020, Proc. SPIE, 11445, 114457F1-114457F13
- [8] Minamidani, T., Nishimura, A., Miyamoto, Y., et al. 2016, Proc. SPIE, 9914, 99141Z
- [9] Taylor, A. R., Gibson, S. J., Peracaula, M., et al. 2003, AJ, 125, 3145
- [10] Miville-Deschenes, M.-A., Murray, N., & Lee, E. J. 2017, ApJ, 834, 57
- [11] Abe, S., Aguasca-Cabot, A., Agudo, I., et al., 2023, A&A, 673, A75.
- [12] Brand J., Blitz L., 1993, A&A, 275, 67
- [13] Reid, M. J., Menten, K. M., Brunthaler, A. et al. 2019, ApJ, 885, 131
- [14] Zabalza V., 2015, ICRC, 34, 922